Design and Simulation of MEMS Electrostatic Resonator for Ammonia Gas Detection Based on SOIMUMPs

SAEED S. BA Hashwan [a], M. H. Md Khir [a], Y Al-Douri [b, c], A. Yousif [a], H. Ramza [d], S. Arjo [d]

[a] Department of Electrical and Electronic Engineering, Universiti Teknologi PETRONAS, 32610 Bandar Seri Iskandar, Perak Darul Rizuan, Malaysia.

[b] Nanotechnology and Catalysis Research Center (NANOCAT), University of Malaya, 50603 Kuala Lumpur, Malaysia.

[c] Department of Mechatronics Engineering, Faculty of Engineering and Natural Sciences, Bahcesehir University, 34349 Besiktas, Istanbul, Turkey.

[d] Universitas Muhammadiyah Prof. Dr. Hamka(UHAMKA), 12130 Jakarta, Indonesia.

2020 8th International Conference on Intelligent and Advanced Systems (ICIAS) | 978-1-7281-7666-6/21/$31.00 ©2021 IEEE | DOI: 10.1109/ICIAS49414.2021.9642706

***Abstract*— The analytical modeling, design, and simulation of micromachined MEMS resonator for ammonia gas detection is presented in this paper. The MEMS resonator is designed to be vibrated electrostatically using interdigitated comb fingers. The demonstrated device is designed to be capable to carry micro-ring resonator and vibrated in-plane laterally to enhance the sensitivity of the gas detection. This MEMS resonator working principle is based on the changes in the output signal wavelength due to the change in the effective refractive index introduced by the ammonia gas. The resonant frequency of the actuator and the pull-in voltage have been calculated theoretically and found to be 11.15 kHz and 79.7 V respectively. The design and simulation of the micromachined micro-resonator has been carried out using CoventorWare software. Furthermore, the mathematically modeled results were verified using the finite element analysis software and the result shows a good agreement within 1.06% error between the modeled and simulated frequencies where the modeled and the simulated frequencies are found to be 11.15 kHz and 11.27 kHz respectively.**

Keywords*— *Micro-Ring Resonator, MEMS, SOIMUMPs, , Analytical modeling, Electrostatic actuation, Transverse, in -plane actuator, Ammonia Gas sensor.

I. INTRODUCTION

In the last decades, many novel gas sensors have been proposed, developed and employed in diverse fields for applications such as industry, environmental analysis, and agricultural production[1][2][3]. Ammonia gas (NH_3) is one of the hazardous gas species that attracted significant attention in the gas sensors development discipline and academia researchers because ammonia is one of the most common chemicals manufactured and used in various application, especially for nitrogen-based fertilizer, cleaning products and petrochemicals production[2][4][5]. Ammonia gas is classified as base and fairly corrosive. It is colorless gas with pungent odor and can be in liquid form when the gas put under enough pressure[6].

According to occupational safety and health administration (OSHA), the exposure limit of NH_3 to human beings is 25 ppm for 8 hours and 35 ppm for 10 minutes. The typical level of the NH_3 gas is in low ppb (1-5 ppb) levels[1]. However, exposing and inhaling more than the safe level of the gas can cause human health problems such as skin, eyes, and lung illness. Therefore, it is important to develop a highly sensitive sensor for the ammonia gas detection.

Currently, there are several techniques for ammonia gas detection including the electrochemical sensing, metal oxide-based sensors, and optical sensors using tunable diode laser spectroscopy[1], [3]–[5], [7]–[9]. Masayasu et al, have developed an optical ammonia gas sensor using silicon micro-ring resonator covered by graphene. They have detected the gas concentration using the micro-ring resonator by the resonant-wavelength shift[10][11].

In this research, we reported a design and develop of SOIMUMPs MEMS actuator to be capable of holding a micro-ring resonator. The micro-ring resonator is used as optical sensor for ammonia gas detection by detecting the changes in the wavelength [12]. In this stay, our objective is to produce the design, simulation and demonstrated the analytical mathematical modeling.

II. MATHEMATICAL MODELING OF THE RESONATOR

The device mathematically modeling has been performed to investigate the natural frequency of the resonator followed by the device simulation to obtain the lateral in-plane oscillation with similar resonant frequency vibrating in the first mode. The micro-ring will be surrounding by Ammonia gas molecules in closed reactor in order to investigate the effect of the ammonia gas in the wavelength change[13].

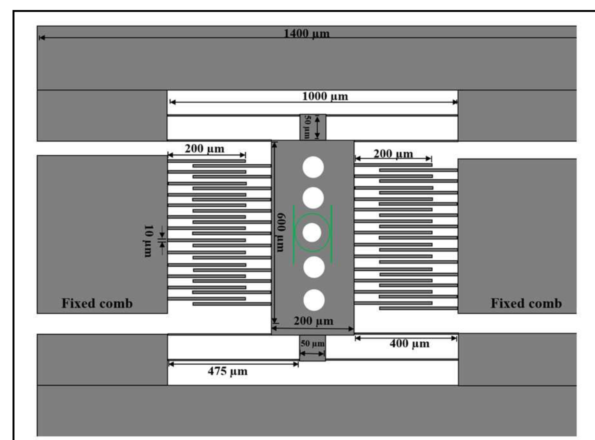

Figure 1: 2-D layout of the SOI-MEMS resonator

XXX-X-XXXX-XXXX-X/XX/$XX.00 ©20XX IEEE

Authorized licensed use limited to: Monash University. Downloaded on January 17,2022 at 07:25:52 UTC from IEEE Xplore. Restrictions apply.

The micro-ring resonator will be attached onto the surface of the MEMS structure to perform as optical gas detector. Fig. 1, shows the device schematic with dimensions of 1400 µm × 1200 µm.

The structure consisted of a suspended shuttle which is attached to the anchors by eight long beams. The shuttle also has 28 fingers which are interdigitated with the stator fingers. Due to the heavy mass of the shuttle, five cylindrical holes have been introduced in the middle of the shuttle in order to reduce the shuttle weight and made it possible for the electrostatic actuator to vibrate the shuttle.

A. Spring constant

The mechanical behavior which is the resonant frequency of the device is investigated and analyzed by calculating the spring constant of the beams. Equation (1) is used to find the mechanical spring constant of the eight beams of the resonator [14][15]:

$$k = 4\left(\frac{Etw^3}{l_1^3}\right) + 4\left(\frac{Etw^3}{l_2^3}\right) \quad (1)$$

where E is the Young's modulus of the silicon beams with the value of 169 GPa, t, w, and L are the thickness, width and length of the beams, respectively. Equation (1), represents the spring constant for the eight beams where L_1 represents the first four beams with different length than the L_2 beams. The beams are considered as parallel beams therefore, the total constant is obtained by a summation relationship.

B. Resonant frequency

The resonant frequency of the resonator is obtained by (2) as

$$f = \frac{1}{2\pi}\sqrt{\frac{k_m}{m_{total}}} \quad (2)$$

where k is the spring constant and can be obtained from (1), while m_{total} is the total mass of the movable parts in the resonator.

Equation (3), is used to find the total mass of the movable parts, which including the mass of the beams, shuttle, junctions and movable beams as shown in (3) as

$$m_{total} = m_{st} + m_{jun} + m_{m-fingers} + m_{m-beams} \quad (3)$$

The equation consists of four sections which are the mass of the shuttle, mass of the junctions, mass of the movable fingers, mass of the movable beams respectively[15]. The junctions are the two small boxes as anchors holding the long beams which can be calculated by (5).

The mass of the shuttle can be calculated using (4)[16], where the p is the silicon material density which is equal to 2330 Kg/m^3. L, w, t, are the length, width, thickness of the shuttle respectively. The shuttle substrate has been modified by introduced five holes inside the shuttle to reduce its weight, thus these modifications have to implemented in (4) to exclude or eliminate the mass of that cylindrical holes. Therefore, the shuttle mass is obtained by

$$m_{shuttle} = plwt - 5(pl\pi R^2)$$

where R is the radius of the design holes in the shuttle.

Furthermore, the mass of the junctions or small anchors are calculated by (5), where h, and w, are the high and width of the two anchors.

$$m_{junction} = 2hw \quad (5)$$

$$m_{fingers} = 28\,plwt \quad (6)$$

Equation (6), shows the method of obtained the mass of the 28 fingers in the device, the p, L, w, t, are the silicon density, beam length, beam width, and thickness respectively.

The mass of the eight movable beams can be calculated by (7), where p, L, w, and t, are the silicon density, length of the beams, width of the beams, and the thickness of the beams respectively.

$$m_{m-beams} = 4(pl_1wt) + 4(pl_2wt) \quad (7)$$

C. Pull-in voltage

The pull-in voltage is the voltage that is required to vibrate the actuator or to make the effective force constant of the spring become zero. If the biasing voltage is increased beyond the pull-in voltage, the two plates in the actuator will be pulled against each other rapidly until it collapse with each other[14][17]. This stay known as snap in. The snap in stay must be avoided in order to maintain the actuator operation. The pull-in voltage is calculated by (8)

$$V_{pull-in} = \frac{2x_\circ}{3}\sqrt{\frac{k_m}{1.5C_\circ}} \quad (8)$$

where x_0, k_m, C_0 are the distance between the two plates, the resonator spring constant, and the capacitance and the pull-in voltage respectively[18]. The capacitance can be obtained by (9)

$$C_\circ = \frac{\varepsilon A}{d} \quad (9)$$

where ε, A, d are the permittivity of the air, the area of the finger plate, and the distance between the two fingers respectively[19].

III. SOI-MEMS Resonator design

The actuator in this research is designed and simulated using CoventorWare finite element analysis (FEA) software. The Actuator is designed layer by layer in the software layout editor including the substrate, thin layer of silicon dioxide, and the specific design of comb fingers, shuttle and beams using the SOI technology [20]. The actuator consists of three layers which is compatible with the SOIMUMPs technology. CoventorWare software provide unique features for MEMS design, meshing and 3D schematic of the device structure.

A. Design details

Table 1 shows the summary of the materials properties and actuator dimensions. The actuator is designed using silicon-on-insulator wafer substrate and using SOI-MEMS

(4)

Authorized licensed use limited to: Monash University. Downloaded on January 17,2022 at 07:25:52 UTC from IEEE Xplore. Restrictions apply.

fabrication process technology by MEMSCAP in the CoventorWare software.

TABLE 1: MATERIAL PROPERTIES AND ACTUATOR DIMENSIONS.

Description	**Value**
Silicon Young's modulus, E	169 GPa
Silicon density, P	2330 Kg/m^3
Shuttle dimension, (W x L)	200 µm x 600 µm
Thickness of movable beams, T_b	25 µm
Width of the movable beams, W_b	5 µm
Length of the outer beams, L_{ob}	475 µm
Length of the beams, L_b	400 µm
Comb fingers length, L_f	200 µm
Comb fingers width, W_f	10 µm
Comb fingers thickness, T_f	25 µm
Gap between right finger, G_{RF}	3 µm
Gap between left finger, G_{LF}	9 µm
Number of comb fingers, N_f	28

B. MEMS resonator structural based on SOI technology

The SOI-MEMS resonator was designed using silicon-on-insulator technology. The SOI-MEMS wafer is consisted of silicon substrate, silicon dioxide as insulator, and silicon layer as conductor. SOI technology has the capability to add one more layer on the silicon surface which are intended to be used as micro-ring resonator[20]. Fig. 2, shows the schematic cross-section of the SOI-MEMS. The shuttle and comb fingers are designed to be fabricated using the silicon layer on the top of the dioxide.

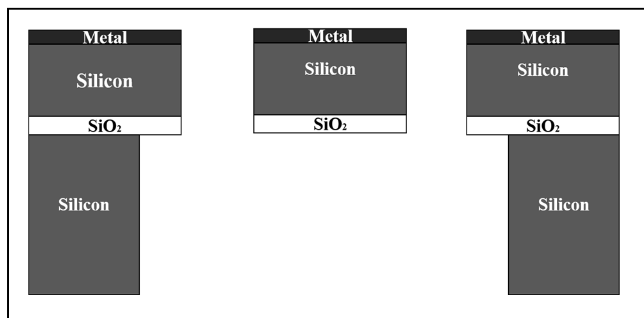

Figure 2: Cross-section of the SOI-MEMS layers.

Fig. 3, shows a 3-D structure of the SOI-MEMS resonator including the shuttle, movable comb fingers, stator comb fingers, and the designed ring-resonator. The structural shows the eight beams that designed to be holding the shuttle with specified dimension. These beams must have unique dimension in order for the resonator to vibrate transverse laterally[15]. The long beams thickness must be more than the width by at least multiplying of 3 times. In this structural, the thickness of the beams is 25 µm and the width was designed to be 5 µm. Furthermore, the distance between the comb fingers are very important to be considered. If one finger surrounding by two other fingers with equal distance, there electrostatic effective will cancel each other and there will be no vibration and movement phenomenon[21]. Therefore, we have designed the distance between the finger to be 3 µm, and 9 µm respectively.

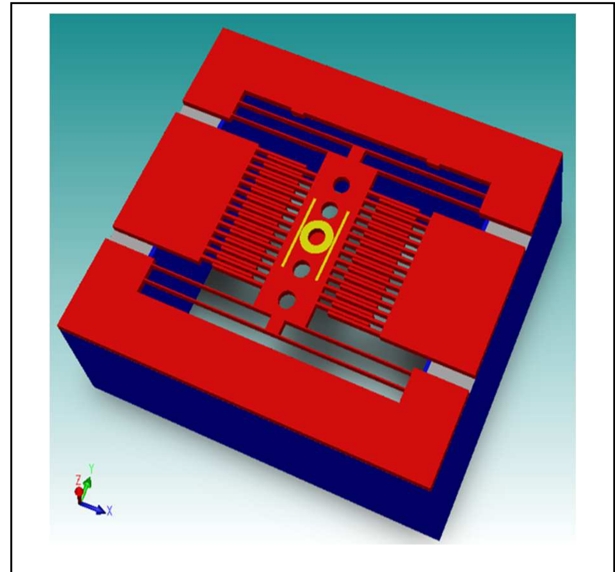

Figure 3: 3-D structure of the SOI-MEMS resonator

IV. SIMULATION RESULTS AND DISCUSSION

The simulations are conducted using mechanical MemMech analysis in the CoventorWare software. After the design is constructed into 3-D structure, surface and face labeling were applied into the resonator to fix the layers. Next, appropriate meshing is applied on the solid model using Tetrahedrons parabolic type mesh structure. The meshing process has been selected to reduce the geometry of the structure to a group of small finite elements and allowed the solver to obtain the finite element method (FEM) analysis. Fig. 4, shows the tetrahedral meshing with 40 µm element mesh size.

After the mesh process was successfully performed, the MemMech solver process is carried out using the analyzer. The analysis has specified to be performed along six different modes.

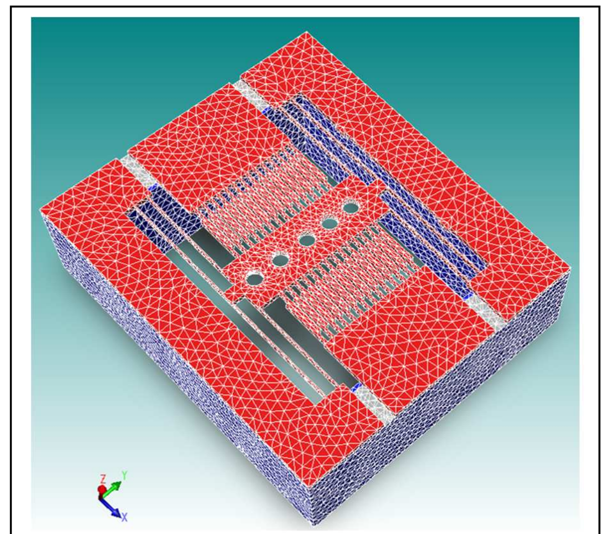

Authorized licensed use limited to: Monash University. Downloaded on January 17,2022 at 07:25:52 UTC from IEEE Xplore. Restrictions apply.

Figure 4: 3-D structure of the meshed resonator

The results show six different modes with resonant frequency of 11.27 kHz, 50.59 kHz, 94.35 kHz, 117.82 kHz, 191.60 kHz, and 191.95 kHz respectively. From the analytical modeling of the resonator, the theoretically calculated resonant frequency was found to be 11.15 kHz which matches with the frequency obtained in the simulation in mode one, the resonant frequency obtained from the simulation is 11.27 kHz. Furthermore, mode one demonstrated the highest displacement of the shuttle in lateral transverse direction.

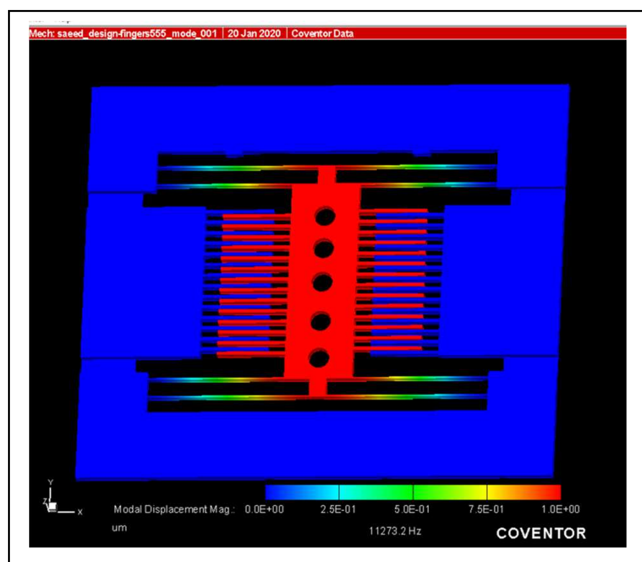

Figure 5: The simulation result of the transverse lateral resonator with lateral displacement and resonant frequency.

The simulation results of the transverse resonator with lateral displacement and the resonant frequency have been successfully demonstrated in Fig. 5. The resonant frequency shown in Fig 5, is the simulated mode one resonant frequency result with frequency of 11.273 kHz. The simulated results have shown the resonator with a good laterally movement and maximum shuttle displacement.

CONCLUSION

In conclusion, in this paper, an electrostatically actuator has been successfully mathematically demonstrated, designed, and simulated using CoventorWare software. The actuator is presented for Ammonia gas detection using SOI-MUMPs fabrication technology. The device has been designed successfully to be capable to carry micro-ring resonator for optical gas detection. The simulated result of the resonator frequency has shown a good agreement with mathematically calculated result. Furthermore, the actuator operation voltage or pull-in voltage has been found to be 79.7 V.

ACKNOWLEDGMENT

This work was supported by Universiti Teknologi PETRONAS under YUTP-FRG Grant number 015LCO-181, and Universitas Muhammadiyah Prof. Dr. HAMKA (UHAMKA) under Grant number 015MEO-068. The authors would like to thank Universiti Teknologi PETRONAS (UTP) and the department of Electrical and Electronic Engineering for providing the research facilities and funding this research.

REFERENCES

[1] B. Timmer, W. Olthuis, and A. Van Den Berg, "Ammonia sensors and their applications - A review," *Sensors Actuators, B Chem.*, vol. 107, no. 2, pp. 666–677, 2005.

[2] D. Kwak, Y. Lei, and R. Maric, "Ammonia gas sensors: A comprehensive review," *Talanta*, vol. 204, no. March, pp. 713–730, 2019.

[3] H. Wu, Z. Ma, Z. Lin, H. Song, S. Yan, and Y. Shi, "High-sensitive ammonia sensors based on tin monoxide nanoshells," *Nanomaterials*, vol. 9, no. 3, 2019.

[4] G. Zhu *et al.*, "Gas sensors based on polyaniline/zinc oxide hybrid film for ammonia detection at room temperature," *Chem. Phys. Lett.*, vol. 665, pp. 147–152, 2016.

[5] Z. Wu *et al.*, "Enhanced sensitivity of ammonia sensor using graphene/polyaniline nanocomposite," *Sensors Actuators, B Chem.*, vol. 178, pp. 485–493, 2013.

[6] R. C. T. Illnesses, "Recognizing Chemical Terrorism-Related Illnesses," *online*, no. July, 2005.

[7] Z. Ye *et al.*, "Excellent ammonia sensing performance of gas sensor based on graphene/titanium dioxide hybrid with improved morphology," *Appl. Surf. Sci.*, vol. 419, pp. 84–90, 2017.

[8] R. Sankar Ganesh *et al.*, "Low temperature ammonia gas sensor based on Mn-doped ZnO nanoparticle decorated microspheres," *J. Alloys Compd.*, vol. 721, pp. 182–190, 2017.

[9] X. Yu, X. Chen, X. Chen, X. Zhao, X. Yu, and X. Ding, "Digital ammonia gas sensor based on quartz resonator tuned by interdigital electrode coated with polyaniline film," *Org. Electron.*, vol. 76, no. August 2019, p. 105413, 2020.

[10] M. Sato, H. Kshikawa, N. Goto, S. I. Yanagiya, and S. K. Liaw, "All-Optical Ammonia Gas Sensor Using Silicon Microring Resonator Covered with Graphene," *2018 Conf. Lasers Electro-Optics Pacific Rim, CLEO-PR 2018*, vol. 2, no. c, pp. 1–2, 2018.

[11] H. Kishikawa, M. Sato, N. Goto, S. I. Yanagiya, T. Kaito, and S. K. Liaw, "An optical ammonia gas sensor with adjustable sensitivity using a silicon microring resonator covered with monolayer graphene," *Jpn. J. Appl. Phys.*, vol. 58, no. SJ, 2019.

[12] D. P. Cai, J. H. Lu, C. C. Chen, C. C. Lee, C. E. Lin, and T. J. Yen, "High Q-factor microring resonator wrapped by the curved waveguide," *Sci. Rep.*, vol. 5, pp. 1–8, 2015.

[13] A. Y. Ahmed, J. O. Dennis, M. H. Md. Khir, and M. N. Mohamad Saad, "Design and simulation of mass-sensitive gas sensor based on CMOS-MEMS resonator," *AIP Conf. Proc.*, vol. 1482, no. September, pp. 673–676, 2012.

[14] J. O. Dennis, A. A. S. Rabih, M. H. Md Khir, M. G. A. Ahmed, and A. Y. Ahmed, "Modeling and Finite Element Analysis Simulation of MEMS Based

Authorized licensed use limited to: Monash University. Downloaded on January 17,2022 at 07:25:52 UTC from IEEE Xplore. Restrictions apply.

Acetone Vapor Sensor for Noninvasive Screening of Diabetes," *J. Sensors*, vol. 2016, no. May, 2016.

[15] L. Zhang and J. Dong, "Design, fabrication, and testing of a SOI-MEMS-based active microprobe for potential cellular force sensing applications," *Adv. Mech. Eng.*, vol. 2012, 2012.

[16] F. J. Ibarra-Villegas, S. Ortega-Cisneros, F. Sandoval-Ibarra, J. J. Raygoza-Panduro, and J. Rivera-Domínguez, "Design of capacitive MEMS transverse-comb accelerometers with test hardware," *Superf. y Vacio*, vol. 26, no. 1, pp. 4–12, 2013.

[17] F. Ahmad, J. O. Dennis, M. H. Md Khir, and N. H. Hamid, "A CMOS MEMS resonant magnetic field sensor with differential electrostatic actuation and capacitive sensing," *Adv. Mater. Res.*, vol. 403–408, pp. 4205–4209, 2012.

[18] O. Pertin and Kurmendra, "Pull-in-voltage and RF analysis of MEMS based high performance capacitive shunt switch," *Microelectronics J.*, vol. 77, no. September 2017, pp. 5–15, 2018.

[19] P. Skrzypacz, S. Kadyrov, D. Nurakhmetov, and D. Wei, "Analysis of dynamic pull-in voltage of a graphene MEMS model," *Nonlinear Anal. Real World Appl.*, vol. 45, pp. 581–589, 2019.

[20] K. Miller, A. Cowen, G. Hames, and B. Hardy, "SOIMUMPs design handbook," *MEMScAP Inc., Durham*, pp. 0–25, 2004.

[21] L. Li and Z. J. Chew, *Microactuators: Design and Technology*. Elsevier Ltd, 2018.

Authorized licensed use limited to: Monash University. Downloaded on January 17,2022 at 07:25:52 UTC from IEEE Xplore. Restrictions apply.

View publication stats